EPR Study of the $[Fe_4S_4]^+$ and $[Fe_4S_4]^{3+}$ States in γ-Irradiated Crystals of $(Bu_4N)_2[Fe_4S_4(SPh)_4]$. $\tilde{g}$ Tensors in Relation to the Geometry of the 4Fe-4S Core

J. Gloux,[†] P. Gloux,*[‡] H. Hendriks,[§] and G. Rius[†]

Contribution from the Centre d'Etudes Nucléaires de Grenoble, DRF/Service de Physique/SCPM, 85 X, 38041 Grenoble-Cedex, France. *Received August 5, 1986*

Abstract: Presented herein are the crystal structure determination of the diamagnetic $(Bu_4N)_2[Fe_4S_4(SPh)_4]$ and the complete EPR study of paramagnetic species created by γ-irradiation of this compound. $(Bu_4N)_2[Fe_4S_4(SPh)_4]$ crystallizes in the monoclinic space group $P2_1/n$ with a = 11.984 (9) Å, b = 23.524 (4) Å, c = 23.686 (3) Å, and β = 91.78 (3)°. The structure of the $[Fe_4S_4]^{2+}$ core shows weak distortions from T_d symmetry which are not describable as a D_{2d} compression. Three paramagnetic species have been identified by EPR spectroscopy; they are believed to correspond to $[Fe_4S_4]^+$ and $[Fe_4S_4]^{3+}$ cores. Here we report the first analysis of the $\tilde{g}$ tensors of such species in relation to the geometry of the $[Fe_4S_4]^{2+}$ core.

In the 4Fe-4S iron-sulfur proteins the active site of the cubane type is generally observed in one or the other of the redox states $[Fe_4S_4]^{2+}$ and $[Fe_4S_4]^+$.[1] The cores of synthetic compounds of the $[Fe_4S_4(SR)_4]^{2-,3-}$ types constitute good analogues for these states and are studied as such.[2] On the other hand, the $[Fe_4S_4]^{3+}$ state is rare[1] and the synthesis of the first analogue of this state is very recent.[3] Antiferromagnetic couplings between the iron ions of formal charges 2+ and 3+ lead to a diamagnetic ground state for the $[Fe_4S_4]^{2+}$ state. Then the states $[Fe_4S_4]^+$ and $[Fe_4S_4]^{3+}$ present a paramagnetic ground state with spin $^1/_2$. Thus, they can be characterized and studied by EPR spectroscopy, and in this case the $\tilde{g}$ tensor constitutes the observable to be measured. EPR studies of proteins[4] or synthetic compounds[5] have been made in frozen solution or in powder form. This has shown that the $[Fe_4S_4]^+$ state had characteristic g values with an average g less than 2. On the other hand, the rarely studied $[Fe_4S_4]^{3+}$ state presented an average g value larger than 2. Evidently, the orientational parameters of the tensors escape analysis.

How can one obtain single crystals of synthetic compounds which will enclose the paramagnetic redox species for obtaining the $\tilde{g}$ tensors in their entirety? Since many compounds have been synthesized in the diamagnetic state on the one hand and since the paramagnetic species are better characterized in a dilute environment on the other hand, Gloux et al. have proposed an original approach to the problem.[6] It consists of studying by EPR single crystals of the diamagnetic species irradiated beforehand with γ-rays, with the hope that the capacity of the iron-sulfur clusters for electronic transfers is correlated with creation of the paramagnetic species during irradiation. They were able to test the method on the synthetic compound[7,8] $(Bu_4N)_2[Fe_4S_4(SPh)_4]$, and they have presented the first results in ref 6. At low temperature the angular dependences for two centers A and B with spin $^1/_2$ could be followed in the three planes ab, bc^*, and c^*a of the monoclinic[9] crystal. The properties of these centers led to their identification with the redox states $[Fe_4S_4]^+$ and $[Fe_4S_4]^{3+}$, respectively, in particular the g values presented the same characteristics. The orientational study was not developed because the correspondence between angular dependences and calculated tensorial solutions was not unique.

Here we present a complementary study in a suitably selected, fourth crystal plane, which allows us to identify the correct tensorial solutions. Also, a new center with spin $^1/_2$ could now be examined, its interest is that it is very much like center B and we shall call it B′. This article gives the complete EPR results for the three centers and includes the analysis of the $\tilde{g}$ tensors in relation to the geometry of the iron-sulfur core. The X-ray structure is reported first below.

X-Ray Data Collection, Solution, and Description of the Structure

A black crystal of $(Bu_4N)_2[Fe_4S_4(SPh)_4]$, of approximate dimensions 0.6 × 0.3 × 0.1 mm, was sealed under argon in a Lindemann capillary. The cell parameters and the space group $P2_1/n$ were determined from diffractometer data at room temperature. Least-squares refinement of the angular settings of 24 reflections with $6° < \theta < 13°$ gave the unit cell dimensions a = 11.984 (9) Å, b = 23.524 (4) Å, c = 23.686 (3) Å, and β = 91.78 (3)°; the calculated density is 1.27 g/cm^3 for Z = 4. Intensity data were collected at ambient temperature on a Nonius CAD-4 diffractometer (ω-scans) for all reflections with $0.5° < \theta < 25°$ and with $h > 0$ and $k > 0$, using graphite-monochromated Mo Kα radiation (λ = 0.7107 Å and μ = 11.8 cm^{-1}). The scanning rate was adjusted to the required precision of $\sigma(I) < 0.02I$ with a maximum scan time of 120 s per reflection. Each reflection was measured in 96 steps. Sixteen steps at each end of the scan were considered as background. Intensities I and their estimated standard deviations $\sigma(I)$ were determined from $I = S[P - 2(B_1 + B_2)]$ and $\sigma(I) = S[P + 4(B_1 + B_2)]^{1/2}$, where S is a factor to account for the variable scan speed, P is the scan count, and B_1 and B_2 are the low- and high-angle background counts. Two standard reflections were measured after every 10800 s of radiation time to check for instrumental instability and crystal decomposition; during the data collection there was a 7% decrease in intensity, for which the data were corrected. The orientation of the crystal was checked after every 100 reflections. Measurement of the intensities of suitable reflections at different azimuthal positions suggested that no absorption correction was necessary. Some 3707 independent reflections were considered as observed ($I > 3\sigma(I)$). The intensities were corrected for Lorentz and

* Author to whom correspondence should be addressed.
† Also at USTM Grenoble, France.
‡ Also at CNRS Grenoble, France.
§ Presently at Dowell-Schlumberger, P.O. Box 90, 42003 St-Etienne, France.

(1) Lovenberg, W., Ed. *Iron-Sulfur Proteins*; Academic Press: New York, 1977; Vol. III.
(2) Berg, J. M.; Holm, R. H. In *Iron-Sulfur Proteins*; Spiro, T. G., Ed.; John Wiley and Sons, Inc.: New York, 1982; Vol. IV, Chapter I.
(3) O'Sullivan, T.; Millar, M. M. *J. Am. Chem. Soc.* **1985**, *107*, 4096.
(4) Cammack, R.; Dickson, D. P. E.; Johnson, C. E. In *Iron-Sulfur Proteins*; Lovenberg, W., Ed.; Academic Press: New York, 1977; Vol. III, Chapter 8.
(5) Holm, R. H.; Ibers, J. A. In *Iron-Sulfur Proteins*; Lovenberg, W., Ed.; Academic Press: New York, 1977; Vol. III, Chapter 7.
(6) Gloux, J.; Gloux, P.; Lamotte, B.; Rius, G. *Phys. Rev. Lett.* **1985**, *54*, 599.
(7) Averill, B. A.; Herskovitz, T.; Holm, R. H.; Ibers, J. A. *J. Am. Chem. Soc.* **1973**, *95*, 3523.
(8) Christou, G.; Garner, C. D. *J. Chem. Soc., Dalton Trans.* **1979**, 1093.
(9) When the temperature is lowered, the crystal system changes from monoclinic to orthorhombic at about 240 K. To prevent this phase transition, the sample is quenched.

0002-7863/87/1509-3220$01.50/0

Table I. Positional Parameters of the Anion of $(Bu_4N)_2[Fe_4S_4(SPh)_4]$ with Their Estimated Standard Deviations in Parentheses

atom[a]	$10^4x/a$	$10^4y/b$	$10^4z/c$
Fe(1)	7324 (2)	2777 (1)	2015 (1)
Fe(2)	9013 (2)	3082 (1)	2765 (1)
Fe(3)	7465 (2)	2283 (1)	3063 (1)
Fe(4)	9014 (2)	2037 (1)	2279 (1)
S(1)	9364 (4)	2247 (2)	3213 (2)
S(2)	7160 (4)	1837 (2)	2208 (2)
S(3)	9165 (4)	2874 (2)	1824 (2)
S(4)	7142 (4)	3211 (2)	2871 (2)
S(10)	6039 (4)	3189 (2)	1431 (2)
S(20)	10224 (4)	3816 (2)	2886 (2)
S(30)	6353 (4)	1800 (2)	3651 (2)
S(40)	10256 (4)	1342 (2)	2089 (2)
C(11)	6174 (23)	2882 (7)	738 (7)
C(12)	7253 (19)	2748 (10)	544 (10)
C(13)	7337 (22)	2509 (11)	−14 (12)
C(14)	6364 (28)	2483 (12)	−346 (11)
C(15)	5297 (24)	2638 (12)	−140 (12)
C(16)	5214 (19)	2811 (10)	398 (11)
C(21)	10313 (18)	3975 (10)	3638 (9)
C(22)	9754 (28)	3699 (12)	4034 (13)
C(23)	9956 (33)	3862 (13)	4598 (14)
C(24)	10594 (33)	4327 (14)	4740 (12)
C(25)	11125 (25)	4609 (16)	4320 (16)
C(26)	11023 (22)	4445 (12)	3765 (12)
C(31)	6367 (20)	2169 (10)	4309 (7)
C(32)	5544 (17)	1971 (11)	4688 (12)
C(33)	5487 (23)	2252 (15)	5230 (14)
C(34)	6210 (30)	2695 (15)	5353 (12)
C(35)	7015 (25)	2905 (11)	4966 (13)
C(36)	7089 (22)	2628 (11)	4438 (11)
C(41)	10058 (22)	1135 (9)	1363 (8)
C(42)	10900 (19)	750 (8)	1157 (12)
C(43)	10794 (30)	566 (12)	576 (14)
C(44)	9815 (34)	766 (14)	257 (13)
C(45)	9028 (25)	1145 (11)	464 (12)
C(46)	9144 (20)	1331 (9)	1026 (11)

[a] The atom numbering scheme is given in Figure 1.

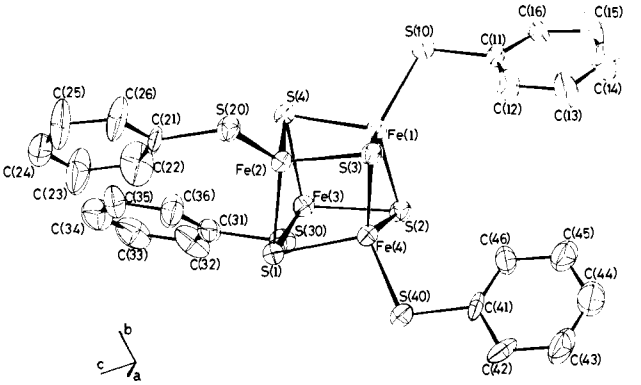

Figure 1. ORTEP drawing of the anion of $(Bu_4N)_2[Fe_4S_4(SPh)_4]$ showing the atom labeling scheme.

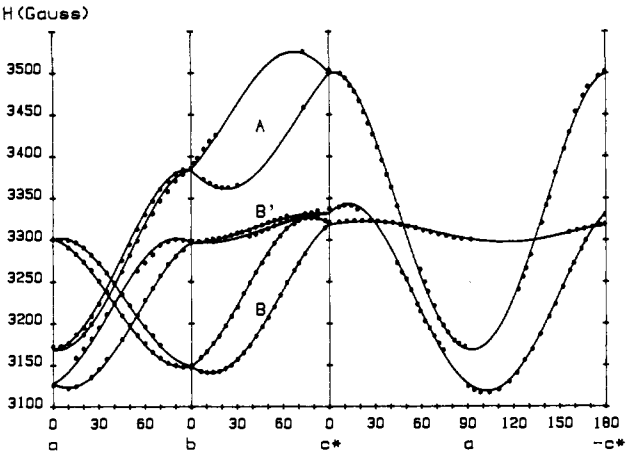

Figure 2. Experimental points and calculated angular dependences of the A, B, and B′ centers in the *ab*, *bc**, and *c***a* planes. Mean microwave frequency is 9.262 GHz.

polarization effects, but not for extinction. Scattering factors for neutral atoms were taken from ref 10, and those for Fe and S were corrected for the real and imaginary parts of anomalous dispersion.[10]

The structure was solved with the direct methods program MULTAN.[11] The solution (based on 397 reflections with $E > 1.50$) with the highest figure of merit revealed the position of the four independent Fe atoms. All other non-hydrogen atoms were found in a series of full-matrix least-squares refinements and subsequent Fourier syntheses. After further refinement, four of the carbon atoms of the tetrabutylammonium ions turned out to be disordered (C(113), C(114), C(134), and C(244)). They were refined in two or three different positions. Values for their multiplicities were suggested by comparison of the thermal parameters. Refinement was completed in several full-matrix least-squares cycles, with anisotropic thermal parameters for the atoms of the $[Fe_4S_4(SPh)_4]^{2-}$ ion and isotropic thermal parameters for the cations. No hydrogen atoms were included. In the last refinement cycle all parameter shifts were less than 0.2 times their standard deviations. A final difference Fourier map revealed no anomalous features. The final residuals are $R = \sum||F_o| - |F_c||/\sum|F_o| = 0.075$ and $R_w = [\sum w(F_o - F_c)^2/\sum w(F_o)^2]^{1/2} = 0.064$; $w = 1/\sigma^2(F_o)$. A list of observed and calculated structure factors is available as supplementary material.

The structure consists of two independent Bu_4N^+ cations and one $[Fe_4S_4(SPh)_4]^{2-}$ anion. The Bu_4N^+ cations are partly disordered and of no interest for this discussion. Their atomic and isotropic thermal parameters and their bond distances and angles are available as supplementary material. The atomic parameters of the anion are listed in Table I; its anisotropic thermal parameters are available as supplementary material. A perspective view of the anion is shown in Figure 1, and its interatomic distances and angles are given in Table II. The atom labeling scheme used for the Fe_4S_4 core corresponds to the one chosen by Holm et al. (Figure 2 of ref 7 and Figure 6 of ref 12). As expected, the geometry of the Fe_4S_4 core is virtually the same as that found for the anion in $(Me_4N)_2[Fe_4S_4(SPh)_4]$.[12] However, careful inspection of all distances and angles (Table II) suggests that the symmetry of the core can no longer be regarded as compressed D_{2d}. Let us choose the axis passing through the top and the bottom faces of the "cube" in Figure 1 as the $\bar{4}$ axis (as in ref 12). As already noticed in ref 6, we find four short and eight long Fe–S* distances in agreement with a compressed D_{2d} symmetry. But the Fe–Fe distances and the S*–Fe–S*, Fe–S*–Fe, and Fe–Fe–Fe angles do not split up according to this D_{2d} symmetry. Taking the axis passing through the left and right face of the "cube" as the $\bar{4}$ axis would not give a clear splitting up of the parameters for the core either.[13] In that case we would have an elongated core with four long and eight short Fe–S* distances instead of the compressed core usually found. The difference of the mean values of the two sets that would be created by a D_{2d} symmetry for each type of parameter is small given the variation within each set. Thus the small deviations from T_d symmetry have to be regarded as random and not as being imposed by a D_{2d} distortion. The present com-

(10) *International Tables for X-ray Crystallography*; Kynoch Press: Birmingham, England, 1974; Vol. IV.
(11) Germain, G.; Main, P.; Woolfson, M. M. *Acta Crystallogr.* **1971**, *127*, 368.
(12) Que, L., Jr.; Bobrik, M. A.; Ibers, J. A.; Holm, R. H. *J. Am. Chem. Soc.* **1974**, *96*, 4168.
(13) Then such a splitting appears for parameters involving atoms outside the core. The S–S distances split up into two long and four short distances and the S–Fe–S* angles split up into four small and eight large angles (Table II). Thus the organic sulfur atoms do not follow the trigonal symmetry found by Carter (Carter, C. W., Jr. *J. Biol. Chem.* **1977**, *252*, 7802).

Table II. Distances (Å) and Angles (deg) for the Anion[a] of $(Bu_4N)_2[Fe_4S_4(SPh)_4]$ with Their Estimated Standard Deviations in Parentheses[b]

Fe–Fe		S*–S*		S*–Fe–S*		Fe–S*–Fe	
Fe(1)–Fe(2)	2.746 (4)	S(1)–S(2)	3.630 (6)	S(3)–Fe(1)–S(4)	104.5 (2)	Fe(3)–S(1)–Fe(4)	72.96 (16)
Fe(3)–Fe(4)	2.726 (4)	S(3)–S(4)	3.609 (6)	S(4)–Fe(2)–S(3)	104.1 (2)	Fe(4)–S(2)–Fe(3)	73.25 (16)
mean	2.736	mean	3.620	S(2)–Fe(3)–S(1)	104.5 (2)	Fe(2)–S(3)–Fe(1)	73.86 (15)
Fe(1)–Fe(3)	2.740 (4)	S(1)–S(3)	3.606 (6)	S(1)–Fe(4)–S(2)	105.4 (2)	Fe(1)–S(4)–Fe(2)	73.86 (16)
Fe(2)–Fe(4)	2.714 (4)	S(2)–S(4)	3.594 (6)	mean	104.6	mean	73.48
mean	2.727	mean	3.600	S(2)–Fe(1)–S(4)	104.2 (2)	Fe(2)–S(1)–Fe(4)	73.07 (15)
Fe(1)–Fe(4)	2.728 (4)	S(1)–S(4)	3.573 (6)	S(3)–Fe(2)–S(1)	104.5 (2)	Fe(3)–S(2)–Fe(1)	73.77 (16)
Fe(2)–Fe(3)	2.749 (4)	S(2)–S(3)	3.562 (6)	S(4)–Fe(3)–S(2)	104.0 (2)	Fe(4)–S(3)–Fe(2)	73.27 (15)
mean	2.739	mean	3.568	S(1)–Fe(4)–S(3)	105.0 (2)	Fe(1)–S(4)–Fe(3)	74.08 (16)
mean of 6	2.734	mean of 6	3.596	mean	104.4	mean	73.55
				S(2)–Fe(1)–S(3)	103.2 (2)	Fe(2)–S(1)–Fe(3)	74.14 (16)
Fe–S		S–S		S(4)–Fe(2)–S(1)	103.4 (2)	Fe(4)–S(2)–Fe(1)	73.86 (16)
Fe(1)–S(10)	2.256 (5)	S(10)–S(20)	6.18	S(1)–Fe(3)–S(4)	103.3 (2)	Fe(1)–S(3)–Fe(4)	74.02 (16)
Fe(2)–S(20)	2.268 (5)	S(20)–S(40)	6.12	S(3)–Fe(4)–S(2)	103.8 (2)	Fe(3)–S(4)–Fe(2)	74.39 (16)
Fe(3)–S(30)	2.265 (5)	S(30)–S(10)	6.19	mean	103.4	mean	74.10
Fe(4)–S(40)	2.267 (5)	S(40)–S(30)	6.15	mean of 12	104.2	mean of 12	73.71
		mean	6.16				
		S(10)–S(40)	6.81	Fe–Fe–Fe		S*–S*–S*	
		S(20)–S(30)	6.91	Fe(3)–Fe(1)–Fe(4)	59.81 (9)	S(3)–S(1)–S(4)	60.4 (2)
		mean	6.86	Fe(4)–Fe(2)–Fe(3)	59.87 (9)	S(4)–S(2)–S(3)	60.6 (2)
				Fe(2)–Fe(3)–Fe(1)	60.04 (9)	S(2)–S(3)–S(1)	60.8 (2)
Fe–S*		S–Fe–S*		Fe(1)–Fe(4)–Fe(2)	60.62 (9)	S(1)–S(4)–S(2)	60.9 (2)
Fe(1)–S(2)	2.268 (5)	S(10)–Fe(1)–S(2)	118.7 (2)	mean	60.09	mean	60.7
Fe(2)–S(1)	2.267 (5)	S(20)–Fe(2)–S(1)	119.4 (2)	Fe(2)–Fe(1)–Fe(4)	59.44 (9)	S(2)–S(1)–S(4)	59.9 (2)
Fe(3)–S(4)	2.263 (5)	S(30)–Fe(3)–S(4)	120.5 (2)	Fe(3)–Fe(2)–Fe(1)	59.83 (9)	S(3)–S(2)–S(1)	60.2 (2)
Fe(4)–S(3)	2.254 (5)	S(40)–Fe(4)–S(3)	118.2 (2)	Fe(4)–Fe(3)–Fe(2)	59.43 (9)	S(4)–S(3)–S(2)	60.2 (2)
mean	2.263			Fe(1)–Fe(4)–Fe(3)	60.33 (9)	S(1)–S(4)–S(3)	60.3 (2)
Fe(1)–S(3)	2.277 (5)	S(10)–Fe(1)–S(3)	118.8 (2)	mean	59.76	mean	60.2
Fe(2)–S(4)	2.284 (5)	S(20)–Fe(2)–S(4)	120.8 (2)	Fe(2)–Fe(1)–Fe(3)	60.13 (9)	S(2)–S(1)–S(3)	59.0 (2)
Fe(3)–S(1)	2.293 (5)	S(30)–Fe(3)–S(1)	119.1 (2)	Fe(4)–Fe(2)–Fe(1)	59.94 (9)	S(4)–S(2)–S(1)	59.3 (2)
Fe(4)–S(2)	2.272 (5)	S(40)–Fe(4)–S(2)	118.8 (2)	Fe(1)–Fe(3)–Fe(4)	59.87 (9)	S(1)–S(3)–S(4)	59.4 (2)
mean	2.282	mean of 8	119.3	Fe(3)–Fe(4)–Fe(2)	60.70 (9)	S(3)–S(4)–S(2)	59.3 (2)
Fe(1)–S(4)	2.286 (5)	S(10)–Fe(1)–S(4)	105.6 (2)	mean	60.16	mean	59.3
Fe(2)–S(3)	2.294 (5)	S(20)–Fe(2)–S(3)	102.5 (2)	mean of 12	60.00	mean of 12	60.0
Fe(3)–S(2)	2.298 (5)	S(30)–Fe(3)–S(2)	103.5 (2)				
Fe(4)–S(1)	2.292 (5)	S(40)–Fe(4)–S(1)	104.2 (2)				
mean	2.293	mean	104.0				
mean of 12	2.279						

	$n = 1$	$n = 2$	$n = 3$	$n = 4$		$n = 1$	$n = 2$	$n = 3$	$n = 4$
S(n0)–C(n1)–C(n2)	119 (2)	125 (3)	114 (3)	115 (3)	S(n0)–C(n1)	1.80 (2)	1.82 (2)	1.78 (2)	1.80 (2)
S(n0)–C(n1)–C(n6)	119 (3)	113 (3)	123 (3)	122 (3)	C(n1)–C(n2)	1.42 (3)	1.34 (3)	1.43 (3)	1.45 (3)
C(n2)–C(n1)–C(n6)	122 (2)	123 (3)	123 (3)	123 (2)	C(n2)–C(n3)	1.44 (3)	1.40 (3)	1.45 (3)	1.44 (3)
C(n1)–C(n2)–C(n3)	118 (2)	117 (3)	117 (3)	118 (3)	C(n3)–C(n4)	1.39 (3)	1.37 (4)	1.38 (4)	1.45 (4)
C(n2)–C(n3)–C(n4)	117 (3)	122 (3)	119 (4)	116 (3)	C(n4)–C(n5)	1.43 (3)	1.37 (4)	1.44 (3)	1.40 (4)
C(n3)–C(n4)–C(n5)	123 (3)	118 (4)	124 (4)	124 (4)	C(n5)–C(n6)	1.35 (3)	1.37 (3)	1.42 (3)	1.40 (3)
C(n4)–C(n5)–C(n6)	120 (3)	122 (4)	118 (3)	119 (3)	C(n6)–C(n1)	1.39 (3)	1.42 (3)	1.41 (3)	1.41 (3)
C(n5)–C(n6)–C(n1)	120 (3)	117 (3)	119 (3)	119 (3)					

[a] The C–C distances for the cations range from 1.42 (3) to 1.68 (7) Å. All distances and angles for the cations are given as supplementary material. [b] S* is used for inorganic sulfur of the core.

pound is the first example of an $[Fe_4S_4(SR)_4]^{2-}$ cluster with no apparent D_{2d} compression of the $[Fe_4S_4]^{2+}$ core.

EPR Results

We recall that, after irradiation at room temperature (a dose of about 2 Mrad with ^{60}Co source), single crystals are examined by EPR at 9 GHz. Saturation of lines at very low temperature and broadening of lines at higher temperature restrict the possibilities of observing the centers to relatively narrow temperature ranges, generally between 15 and 50 K.[9] As well as the A, B, and B′ signals, other signals appeared around $g = 2$ but the data collected were too incomplete to be usable. Figure 2 presents the angular dependences of center B′ in the planes ab, bc^*, and c^*a; we recall also the angular dependences of centers A and B already given in ref 6. The points correspond to the experimental values of the transitions and the continuous curves correspond to the fit based on a Zeeman interaction $\vec{H}\tilde{g}\vec{S}$ with a spin $^1/_2$, which leads to two series of possible tensorial solutions for each center. Table III presents the solutions designated 1 and 2, in the system of axes $\vec{a},\vec{b},\vec{c}^*$, for a site of each center.

It was then necessary to find a fourth plane in which, for each center, the two series of solutions would give sufficiently distinct calculated angular dependences. The comparison with the experimental angular dependences would then allow identification of the correct solutions. The morphology of the crystal, a thin plate perpendicular to the axis $\vec{c}^*$, oriented our choice to a plane containing $\vec{c}^*$. After inspection of calculated angular dependences for a sampling of planes of this type, the plane c^*x with $\vec{x}$ in the plane ab at 65° from $\vec{a}$ and at 25° from $\vec{b}$ appeared to offer good prospects for resolving the problem. The experimental angular dependences could be obtained and are represented by the points in Figure 3. This allowed us to select the particular series of tensorial solutions giving rise to the calculated dependences plotted as continuous curves; thus, in all three cases, we keep solution 1 of Table III.

$\tilde{g}$ Tensors in Relation to the Geometry of the Iron–Sulfur Core

We shall not restate the arguments, based on the similarity of behavior as a function of temperature and on the similarity of the g values, which were developed in ref 6 to support the hypothesis that these centers constitute analogues of $[Fe_4S_4]^+$ and $[Fe_4S_4]^{3+}$ states of protein active sites, trapped in the iron–sulfur core of the synthetic compound. As regards the structure of centers, we lack points of comparison with paramagnetic active species. Therefore we can only use the above structural data of the compound and we have tried to establish connections between the paramagnetic centers and the diamagnetic "cube", which, as we have seen, has a structure rather close to T_d symmetry, in this monoclinic crystal. Indeed, it is with the iron–sulfur core itself that we find significant relations for the sets of the principal

Table III. $\tilde{g}$ Tensors of Centers A, B, and B′ in the System of Axes $\vec{a}$, $\vec{b}$, $\vec{c}^*$

center	solution	g values		direction cosines with respect to: $\vec{a}$	$\vec{b}$	$\vec{c}^*$
A	1	2.090	$\vec{V}_1$	0.9973	−0.0485	−0.0545
		1.968	$\vec{V}_2$	0.0656	0.9229	0.3794
		1.877	$\vec{V}_3$	0.0319	−0.3820	0.9236
	2	2.089		0.9987	−0.0261	−0.0428
		1.969		0.0076	0.9226	−0.3857
		1.877		0.0495	0.3849	0.9216
B	1	2.005	$\vec{V}_1$	0.9721	−0.1283	−0.1961
		2.108	$\vec{V}_2$	0.0857	0.9734	−0.2123
		1.988	$\vec{V}_3$	0.2182	0.1896	0.9573
	2	2.007		0.9318	0.0151	−0.3625
		2.108		0.0645	0.9763	0.2065
		1.986		0.3571	−0.2158	0.9088
B′	1	2.125	$\vec{V}_1$	0.9673	−0.1509	−0.2039
		2.006	$\vec{V}_2$	0.0990	0.9647	−0.2440
		1.978	$\vec{V}_3$	0.2335	0.2159	0.9481
	2	2.125		0.9656	−0.1568	−0.2074
		2.005		0.1345	0.9839	−0.1180
		1.979		0.2225	0.0860	0.9711

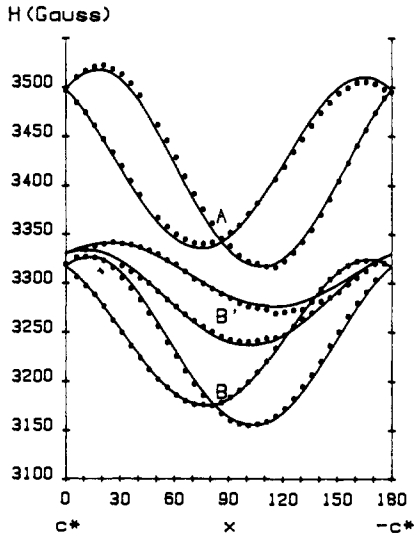

Figure 3. Experimental points and calculated angular dependences of the A, B, and B′ centers in a c^*x plane ($\tilde{x}$ in the ab plane at 65° from $\vec{a}$ and 25° from $\vec{b}$). Mean microwave frequency is 9.257 GHz.

directions of the $\tilde{g}$ tensors. Subsequently, when we talk of symmetry, symmetry elements, or equivalence between ions in the "cube", it is evidently always implied that these concepts are only approximate.

The $\tilde{g}$ Tensor of Center A. In preamble to the analysis of the rhombic tensor of center A, we notice that the arrangement in the crystal unit cell is such that diamagnetic "cubes" related by the screw axis or the glide plane enclose practically identical sets of three significant nearly orthogonal directions: the set **X** constituted by the directions $\overrightarrow{Fe_1Fe_3}\times\overrightarrow{Fe_2Fe_4}$, $\overrightarrow{Fe_4Fe_2}$, $\overrightarrow{Fe_1Fe_3}$ and the set **Y** constituted by the directions $\overrightarrow{Fe_1Fe_3}\times\overrightarrow{Fe_2Fe_4}$, $\overrightarrow{Fe_1Fe_2}\times\overrightarrow{Fe_3Fe_4}$, $\overrightarrow{Fe_1Fe_4}\times\overrightarrow{Fe_3Fe_2}$ normal to the "cube faces" (S could be substituted for Fe here since the $\overrightarrow{S_iS_j}$ and $\overrightarrow{Fe_iFe_j}$ directions are practically parallel). Subsequently, the "cube" of which the structure is reported above is named I and a homologue obtained by the screw axis operation or the glide reflection is named II. Table IV gives the direction set **X**(I) (the set **X** for "cube" I) and the direction set **Y**(II) (the set **Y** for "cube" II) in the system of axes $\vec{a}$, $\vec{b}$, $\vec{c}^*$. Now we can remark that the directions $\vec{V}_1$, $\vec{V}_2$, $\vec{V}_3$ of the A tensor in Table III lie close to these directions, deviating by about 3–5° with respect to the directions **X**(I) and 2–3° with respect to the directions **Y**(II).

Table IV. The Direction Sets **X** for "Cube" I and **Y** for "Cube" II in the System of Axes $\vec{a}$, $\vec{b}$, $\vec{c}^*$

	direction cosines with respect to: $\vec{a}$	$\vec{b}$	$\vec{c}^*$
X(I)			
$\overrightarrow{Fe_1Fe_3}\times\overrightarrow{Fe_2Fe_4}$	0.9993	0.0265	−0.0246
$\overrightarrow{Fe_4Fe_2}$	−0.0136	0.9056	0.4239
$\overrightarrow{Fe_1Fe_3}$	0.0335	−0.4239	0.9051
Y(II)			
$\overrightarrow{Fe_1Fe_3}\times\overrightarrow{Fe_2Fe_4}$	0.9993	−0.0265	−0.0246
$\overrightarrow{Fe_1Fe_2}\times\overrightarrow{Fe_3Fe_4}$	0.0406	0.9412	0.3353
$\overrightarrow{Fe_1Fe_4}\times\overrightarrow{Fe_3Fe_2}$	0.0071	−0.3452	0.9385

Whatever the connection may be, the A tensor principal direction $\vec{V}_1$ that corresponds to the highest principal value has the property of being almost normal to a "cube face". This finding suggests a C_2 symmetry for center A trapped in the "cube", with the twofold rotation axis normal to a "cube face". The closeness of the set of the three directions $\vec{V}_1$, $\vec{V}_2$, $\vec{V}_3$ to one or other set of significant directions could suggest an even higher symmetry than C_2 symmetry: a C_{2v} symmetry in the case **X**(I) and a D_2 symmetry in the case **Y**(II).

For center A in D_2 symmetry the four irons would all appear equivalent. For center A in C_2 or C_{2v} symmetry the irons would appear equivalent only two by two: Fe_1 and Fe_3 on the one hand, Fe_2 and Fe_4 on the other hand. The latter possibility would agree with the observations in the proteins. Indeed, in the $[Fe_4S_4]^+$ state of the protein active site, the rhombic set of g values shown by the EPR studies is associated with irons equivalent two by two, as shown by the "Mössbauer" studies.[4]

The $\tilde{g}$ Tensors of Centers B and B′. The axial tendency is marked for the tensors of centers B and B′ (Table III). But, in consideration of the similarity of the two sets of principal values, the aspect which must be first emphasized is that we have here two centers of the same type which would have to be arranged in relatively equivalent orientations in the crystal. This property would have to appear in the tensor principal directions having similar principal values, i.e., for the direction pairs $(\vec{V}_1,\vec{V}_2)$, $(\vec{V}_2,\vec{V}_1)$, $(\vec{V}_3,\vec{V}_3)$ of the (B,B′) tensors, and in this respect the pair of $g_\parallel$ directions $(\vec{V}_2,\vec{V}_1)$ has to be particularly significant. To find a priori rather equivalent orientations requires that the two sets of tensorial directions be connected with "cube" I.

The principal directions having the same index are very close to each other; in the three cases the differences are about 1.5–2°. For simplicity, we pretend that similar principal values as well as directions having the same index are identical: conversion of the B and B′ tensors into each other is achieved by permutation of principal values of directions $\vec{V}_1$ and $\vec{V}_2$, i.e., by a rotation of 90° about direction $\vec{V}_3$ or by a rotation of 180° about one or the other bisector of the directions $\vec{V}_1$ and $\vec{V}_2$. Among the symmetry elements which may be present in the diamagnetic "cube", none achieves this operation well, which is quite natural since the symmetry elements are only approximate. What is strange on the other hand is the resemblance of the two sets of directions; we must consider this as a combination of circumstances, exceptional though it may be. Reflection in the plane $Fe_1Fe_4S_1S_4$, which is almost parallel to the directions $\vec{V}_3$ (with deviations of about 2 and 3.5°), appears to be an acceptable solution to the conversion problem: the direction $\overrightarrow{Fe_2Fe_3}$, which can be assimilated to the normal of this plane, deviates less than 8° with respect to one of the above bisectors.

For the B and B′ tensors, the directions $\vec{V}_1$, $\vec{V}_2$, $\vec{V}_3$ make angles of 10–15° with the directions **Y**(I) normal to the "cube faces" in "cube" I. More specifically, the directions corresponding to the highest principal values $g_\parallel$, $\vec{V}_2$ for center B and $\vec{V}_1$ for center B′, make angles of respectively 10° with the direction $\overrightarrow{Fe_1Fe_2}\times\overrightarrow{Fe_3Fe_4}$ and 15° with the direction $\overrightarrow{Fe_1Fe_3}\times\overrightarrow{Fe_2Fe_4}$. In comparison with the rhombic A tensor, the principal directions deviate more from significant directions, while in return the axial tendency is well marked. The departures of the $g_\parallel$ directions from normals to "cube

faces" and the deviations from axiality are restricted, which suggests a certain tetragonal symmetry character. For centers B and B' according to this model, the four irons would appear equivalent up to a point. In the $[Fe_4S_4]^{3+}$ state in Chromatium HiPIP protein, the EPR spectrum is considered as axial within the accuracy of the "powder" measurements[4] but the fits of the "Mössbauer" spectra are realized with two types of irons.[14] Connection with centers B and B' is not straightforward.[15]

Conclusion

In this article we have presented the $\tilde{g}$ tensors of species created by γ-irradiation that we believe to be paramagnetic forms of 4Fe-4S "cubes". We have discussed the relations between the tensorial directions and the structure of the diamagnetic "cube", and we have proposed plausible assumptions to account for the results. This study is simply the first of this kind. In other compounds where the "cube" would be arranged in a different way in the crystal unit cell, one should not have certain ambiguities that we have encountered here. A true appreciation of the paramagnetic species considered will be provided by comparison between EPR results of various compounds.

Acknowledgment. We are grateful to Dr. R. Cox and Dr. J. Laugier for helpful discussions.

Registry No. $(Bu_4N)_2[Fe_4S_4(SPh)_4]$, 52586-83-1.

Supplementary Material Available: Tables of positional parameters and isotropic thermal parameters of the cations (Table SII), bond distances and angles of the cations (Table SIII), and anisotropic thermal parameters of the anion (Table SIV) (3 pages); a list of observed and calculated structure factors (20 pages). Ordering information is given on any current masthead page.

(14) Middleton, P.; Dickson, D. P. E.; Johnson, C. E.; Rush, J. D. *Eur. J. Biochem.* **1980**, *104*, 289.

(15) Lattice effects can distort the Fe_4S_4 "cubes" in the analogue clusters in different ways. Furthermore, as emphasized by one referee, the structures and distortions in the radiation generated centers are not known. Thus, the greatest care must be taken in comparing protein paramagnetic active sites with paramagnetic centers created in synthetic crystals.

A Dynamic ^1H NMR and ab Initio MO Investigation of the Barrier to Pyramidal Inversion in Azetidine

Remo Dutler, Arvi Rauk,* and Ted S. Sorensen

Contribution from the Department of Chemistry, The University of Calgary, Calgary, Alberta, Canada T2N 1N4. *Received November 24, 1986*

Abstract: Conformational interconversion in azetidine was investigated by low-temperature ^1H NMR spectroscopy and ab initio molecular orbital theory. Coalescence of the α- and β-proton signals was observed with $\Delta G^{\ddagger}$ (154 K) = 30 kJ mol^{-1}. Analysis of changes in the line shape yielded $\Delta H^{\ddagger} = 21 \pm 4$ kJ mol^{-1} and $\Delta S^{\ddagger} = -45 \pm 25$ J mol^{-1} K^{-1}. Three stationary points were located using RHF theory and analytical gradient techniques at the 6-31G** basis set level. Harmonic frequency analysis was used to characterize two as equivalent minima, a puckered ring with an equatorial N-H bond, separated by the third, a transition structure with C_{2v} symmetry, and to provide an estimate for zero-point vibrational energy (ZPVE) corrections to the barrier to nitrogen inversion. The computations confirm the low measured value for the nitrogen inversion. A value of 27.1 kJ mol^{-1} is obtained after inclusion of correlation corrections up to third order in Moller-Plesset perturbation theory (MP3), and taking account of ZPVE differences. Parallel calculations on aziridine and ammonia yield values of 77.9 and 22.3 kJ mol^{-1}, respectively, for the barrier to pyramidal inversion.

The effect of angular constraint on barriers to pyramidal inversion at tricoordinated atomic centers has been well documented for a variety of atoms[1] and in particular for nitrogen.[2] Barriers hindering pyramidal inversion at tricoordinated N substituted by alkyl groups or hydrogen atoms in systems without constraints at the inverting center have been found experimentally to fall in the range 16 to 30 kJ mol^{-1}. This group of amines is typified by ammonia, whose inversion barrier has been measured[3] at 24.1 kJ mol^{-1}. It has been demonstrated that ab initio calculations *at the RHF level* are able to reproduce this value accurately provided that a large polarized basis set is employed.[4,5] If one of the angles at the inverting center is fixed (as in a small ring) at a small value, the barrier to inversion is increased. The barrier to inversion in aziridine has been observed by gas-phase NMR to be 79.9 kJ mol^{-1} after correction for zero-point vibrational energy differences ($\Delta G^{\ddagger}$ = 72.1 kJ mol^{-1}, 338 K).[6] The inversion barriers in 1-methylaziridine and 1,2,2-trimethylaziridine in solution have been shown to have similar values, $\Delta G^{\ddagger} = 79$[7,8] and $= \sim 77$ kJ mol^{-1},[9] respectively, suggesting that N-alkylation does not have a dramatic effect on the barrier to inversion. As the barriers to inversion in 1-methylazetidine and 1,3,3-trimethylazetidine had been shown to be 42[10] and 34 kJ mol^{-1},[11] respectively, the recent report[12] that the inversion barrier in azetidine, measured in the gas phase by NMR spectroscopy, is 75 kJ mol^{-1} came as a surprise,[13] especially

(1) For a review, see: Rauk, A.; Allen, L. C.; Mislow, K. *Angew. Chem., Int. Ed. Engl.* **1970**, *9*, 400-414.

(2) (a) Lehn, J.-M. *Fortsch. Chem. Forsch.* **1970**, *15*, 311-377. (b) Lambert, J. B. *Top. Stereochem.* **1971**, *6*, 19-105.

(3) Swalen, J. D.; Ibers, J. A. *J. Chem. Phys.* **1962**, *36*, 1914-1918.

(4) (a) Rauk, A.; Allen, L. C.; Clementi, E. *J. Chem. Phys.* **1970**, *52*, 4133-4144. (b) Stevens, R. M. *Ibid.* **1971**, *55*, 1725-1729.

(5) Rodwell, W. R.; Radom, L. *J. Chem. Phys.* **1980**, *72*, 2205-2206.

(6) (a) Carter, R. E.; Drakenberg, T.; Bergman, N. A. *J. Am. Chem. Soc.* **1975**, *97*, 6990-6996. (b) Borchardt, D. B.; Bauer, S. H. *J. Chem. Phys.* **1986**, *85*, 4980-4988. (c) Nakanishi, H.; Yamamoto, U. *Tetrahedron*, **1974**, *30*, 2115.

(7) Gutowsky, H. S. *Ann. N.Y. Acad. Sci.* **1958**, *70*, 786-805.

(8) Heeschen, J. P. Ph.D. Thesis, Univerisy of Illinois, 1959.; *Diss. Abstr.* **1960**, *20*, 3090-3091.

(9) Jautelat, M.; Roberts, J. D.; *J. Am. Chem. Soc.* **1969**, *91*, 642-645.

(10) Lambert, J. B.; Oliver, W. L., Jr.; Packard, B. S. *J. Am. Chem. Soc.* **1971**, *93*, 933-937.

(11) Lehn, J.-M.; Wagner, *J. Chem. Soc., Chem. Commun.* **1968**, 148-150.

(12) Friedman, B. R.; Chauvel, J. P., Jr.; True, N. S. *J. Am. Chem. Soc.* **1984**, *106*, 7638-7639.

0002-7863/87/1509-3224$01.50/0